



International Conference on Sustainable Materials Processing and Manufacturing, SMPM 2017,
23-25 January 2017, Kruger National Park

Determination of Residual Stresses in Roll Compacted Titanium Strips

K. L. Mothosi^a, S. Chikosha^{b*}, D. M. Madyira^a and H. K. Chikwanda^b

^aMechanical Engineering Science Department, University of Johannesburg, South Africa

^bPowder Metallurgy technologies, Light metals, Materials Science and Manufacturing, (CSIR), Pretoria, 0001, South Africa

Abstract

Manufacturing processes typically produce residual stresses. The residual stresses can be advantageous when they are compressive and detrimental when tensile. In roll compaction of metal powder, similarly to rolling solid metals, substantial residual stresses can be generated. In roll compaction of metal powders, few studies have been done to identify the presence of any residual stresses, their effects on the process that produced them and subsequent processes. In this study, residual stress induced during roll compaction of titanium strips were measured for strips of different densities. The different densities were achieved by rolling two different particle size (100 and 325 mesh) titanium powders varying the roll gap (0.1, 0.3 and 0.5mm) and the set strip width (20, 50, 100 mm). The roll speed was kept constant at 10 rpm while three feed rates were employed i.e. 15 g/s for 20mm strip width, 30 g/s for 50mm strip width, and 60 g/s for 100mm strip width. The strips were evaluated for surface residual stresses using x-ray diffraction (XRD) surface probing technique. Preliminary results were obtained for the surface residual stress at the center of the titanium strips for the 100 and 325 mesh strips rolled at 0.1 roll gap for 20 and 50mm set width. Results show the presence of largely compressive residual stresses. The largest surface residual stress of -55 MPa was recorded corresponding to a compaction density of 83 %. The corresponding maximum shear stress was 27 MPa. Lower green density resulted in progressively more tensile residual stresses although all stresses remained compressive for the investigated parameters.

© 2017 The Authors. Published by Elsevier B.V. This is an open access article under the CC BY-NC-ND license (<http://creativecommons.org/licenses/by-nc-nd/4.0/>).

Peer-review under responsibility of the organizing committee of SMPM 2017

Keywords: Titanium powders; density; Residual stress; X-ray diffraction

1. Introduction

Titanium metal is known for its high strength-to-weight ratio advantage over other structural materials like steel and light metals such as aluminum [1, 2]. It also has other excellent properties such as good corrosion resistance and biocompatibility. This makes it favorable for use in many applications. However, this material finds use mostly in applications such as aerospace or medical and minimal use in other applications. This is due to the high cost of the titanium metal. This high cost is due to difficulties associated with the processing/extraction of titanium and the machining of the metal [3]. Alternative low cost processing methods that can reduce the cost of titanium would improve the application of titanium in more widespread industries.

Powder metallurgy is a process that is known to reduce costs [4, 5]. This is due to its ability to make near net or net shape components with minimal or no machining requirements. There are several powder metallurgy techniques such as press and sinter (P & S), metal injection molding (MIM), extrusion, forging, direct powder rolling (DPR) and others. These processes offer different advantages such as production of net shapes that are small and complex in bulk quantities such as in MIM and semi-finished flat products such as plates, sheets and strips as obtained in DPR. Direct powder rolling (DPR) is a powder metallurgy process that can be used to make flat mill products such as plates, sheets, coils and strips [6, 7, 8]. This process involves several stages and currently two routes are known. One route involves roll compaction, thermal treatments/sintering and post sintering treatment such as cold rolling and/or annealing (ADMA) [9]. The other route includes roll compaction, thermomechanical treatments/hot rolling and post hot rolling treatment such as cold rolling and/or annealing [7, 8]. The roll compaction stage is a critical stage in regards to achievement of full density and dimensional stability of the compacts during roll compaction and in the subsequent processing stages. High green densities assist in achieving full density without applying extreme thermal or thermomechanical conditions. Dimensional stability assists with the retention of 'flatness' for the strips during processing. Dimensional distortions can be caused by differing shrink rates due to varying densities within a strip during thermal treatments. They can also be caused by residual stresses induced by the manufacturing process or relaxation of the residual stresses during thermal processing [11-17].

Residual stresses can be defined as stresses that remained locked up in a component after processing and all externally imposed loading has been removed [18]. Processes that can introduce residual stresses include mechanical, thermal, and chemical processes. Mechanically generated residual stresses are due to manufacturing processes that produce non-uniform plastic deformation. They can develop naturally during processing or introduced to attain particular stress profiles in a component. Thermally generated residual stresses are due to non-uniform heating or cooling. In large components this can lead to severe thermal gradients and the development of large internal stresses. The chemically generated stresses can develop due to volume changes associated with chemical reactions, precipitation, or phase transformation.

There are several techniques that can be used to study residual stresses in a component. These range from the destructive techniques to nondestructive techniques. The mechanical stress measurement methods include Curvature Analysis, Hole Drilling [19] and Compliance Methods. There is also magnetic and electrical methods, ultrasonic methods, thermoelastic methods, photo elastic methods, and diffraction methods such as neutron diffraction, synchrotron diffraction and X-ray diffraction [20-21]. Nondestructive diffraction stress measurement in general is based on probing the lattice plane separation distance in a material which depends on the applied loading. This translates to induced strain when compared to the stress free lattice plane separation distance. The XRD method specifically measures the average stress for depth levels of 5 - 7 μm due to limited energy levels. However, for assessment of surface stresses, this is adequate.

Roll compaction is a mechanical process which can result in residual stresses if non uniform deformation occurs. There are few studies that have been carried out to understand residual stresses induced in roll compaction, hence efforts to study this area would be beneficial. Researchers showed that alligatoring during roll compaction of powders can occur due to residual stresses [22]. Other researchers have stated that variations in residual stresses can lead to distortions in subsequent sintering process [14-17]. Consequences of these residual stresses can lead to defects or loss of flatness of the strips. It is important to determine the presence of residual stresses in the roll compacted strips. In this study, the presence of residual stresses on roll compacted strips was investigated and how they vary with compaction density. Preliminary measurements were done at the center of the strips for the 100 and 325 mesh powders rolled at 0.1 roll gaps with a set width of 20 and 50mm.

2. Methodology

2.1. Aim of the Investigation

The study was carried out to determine the presence of residual stresses and how they vary with compaction density.

2.2. Materials

Compacts were prepared from titanium powder produced by the hydrogenation-dehydrogenation (HDH) process. This powder is favorable for consolidation. The TiHDH powder was used in two mesh sizes i.e. 100 and 325 mesh. The chemical composition of the powder as per manufacturer specifications are shown in Table 1.

Table 1: Chemical compositions (by weight) of TiHDH 100 and 325 mesh powder

	O ₂	N ₂	H ₂	C	Cl	Fe	Si	Mn	Ti
Ti HDH 100 mesh	0.18	0.025	0.03	0.02	0.04	0.035	0.02	0.01	Bal.
Ti HDH 325 mesh	0.26	0.025	0.03	0.02	0.04	0.035	0.02	0.01	Bal.

2.3. Experimental procedures

2.3.1. Roll compaction

Rolling was carried out using a modified Schwabenthal T150 rolling mill with a roll diameter of 170mm. The powders were fed into horizontally aligned rolls using a conical hopper with varying openings for different feed rates. The strip widths were set by confining the sides using adjustable side plates made of stainless steel. The strip widths were varied at 20, 50 and 100 mm and the roll gap set at of 0.1, 0.2 and 0.3mm. The speed was set at 10rpm. The green strips were cut into 100mm length and five of the 100 mm long strips were measured for density by measuring the mass and the dimensions. The mass was measured using an Ohaus Explorer balance and the width and length of the strips measured with a Vernier calliper. The thickness of the strips was measured by a micrometre screw gauge. For all the dimensions, averages of 5 values per dimension were used.

2.3.2. Residual Stress Measurement

The prepared samples were then characterised for residual stresses using the XRD machine at the Nuclear Energy Corporation of South Africa (Necsa). Residual stress measurements were conducted using a Bruker D8 X-Ray Diffractometer (XRD). The machine operated in two-dimensional XRD reflective geometry mode incorporating an Eulerian cradle and employing a Hi-star detector and a Cu-K α (0.154055 nm) tube. The recording range was 20-125° and step size was 0.04°. The diffraction plane was (213), the Young's modulus was 112.99 GPa and the Poisson's ratio was 0.32.

3. Results and discussion

Figure 1 (a) and (b) show the scanning electron micrographs of the TiHDH 100 mesh and 325 mesh powders, respectively. The micrographs show irregular shaped powder particles with a hint of sponginess. The 100 mesh powders have a larger particle size with a D90 of 134 μ m and the 325 mesh have a finer particle size with a D90 of 43 μ m. The 100 mesh powder has an O₂ content of 0.18% and the 325 mesh has O₂ content of 0.26% equivalent to commercially pure CP Ti grade 1 and CP Ti grade 2 compositions respectively.

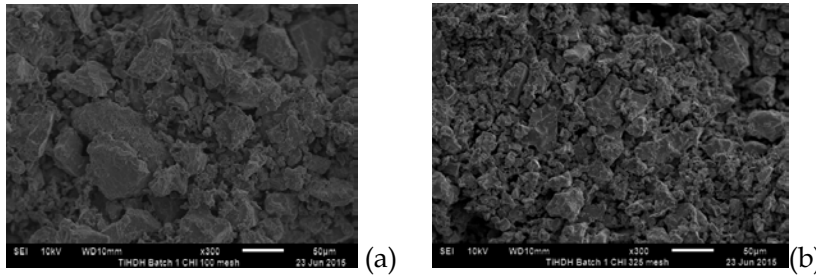


Figure 1: Scanning electron micrographs (SEM) of TiHDH (a) 100 mesh powder and (b) 325 mesh powder

Table 2 shows the green densities (%) obtained for both powders. The densities were highest for the coarse 100 mesh powder at small roll gaps and small set widths. The samples whose densities are highlighted in colour were the ones that were analysed for residual stress.

Table 2: Densities (%) for changing roll gap and set width for TiHDH Batch 1 CHI 100 mesh (-150µm) and 325 mesh (-45µm)

Roll gap Set width	0.1 mm		0.3 mm		0.5 mm	
	100 mesh	325 mesh	100 mesh	325 mesh	100 mesh	325 mesh
20mm	83	79	83	64	74	DNR
50mm	77	66	75	DNR	67	DNR
100mm	74	63	72	ND	ND	ND

DNR – Did not roll

ND – Condition not tested due to the possibility that the strip was not going to be strong enough to hold based on previous DNR experiments

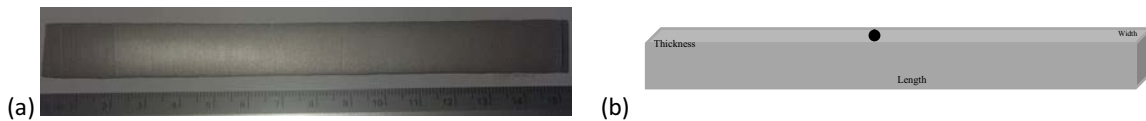


Figure 2: (a) Photographs of a typical green strip (b) Schematic showing the position at which RS was measured.

Figure 3a shows the variation of density for the 100 mesh strip rolled at 0.1 mm roll gap for the 20, 50 and 100mm wide strips. The density is seen to decrease with increasing strip width. Figure 3b shows the corresponding residual stresses for the 20 and 50mm wide strips. The z component stresses (normal to the surface) are seen to be zero as expected due to the prevailing boundary conditions. The x and y components are all seen to be compressive. However, a decrease in density is shown to cause a reduction in the magnitude of the stresses although they remain compressive. Figure 4a shows the variation of density for the 325 mesh strip rolled at 0.1 roll gap for the 20, 50 and 100 mm wide strips. The density decreased with increasing strip width and the maximum density was observed to be lower than that of the 100 mesh rolled strip for similar conditions. This decrease in mesh size leads to reduced compaction density. Figure 4b shows the residual stresses recorded for the 325 mesh strips. Residual stress profiles for this powder size are similar to those observed for the 100 mesh strips. However, the stress levels were larger in magnitude for the 100 mesh strips compared to the 325 mesh strips. This suggests a direct correlation between the compaction density and the residual stress magnitude.

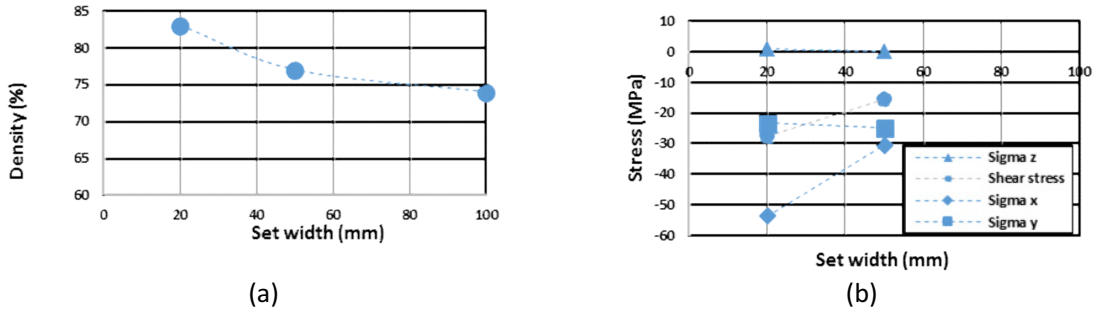


Figure 3: (a) Density and (b) Residual principal and shear stresses for 100 mesh powder rolled at 0.1mm roll gap at set width of 20 and 50mm

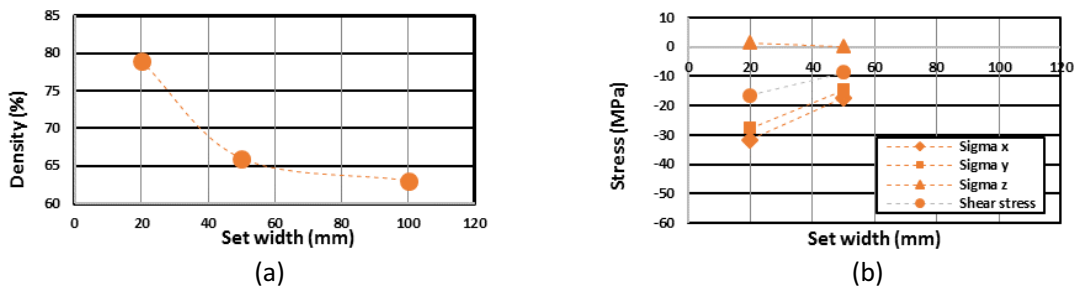


Figure 4: (a) Density and (b) Residual principal and shear stresses for 325 mesh powder rolled at 0.1 mm roll gap at set width of 20 and 50 mm

The principal residual stresses for the stress states shown in Figure 3(a) and Figure 4(a) are presented in Figure 5 as a function of compaction density. The results show that of the important normal stresses (Sigma 1 and Sigma 2) one is tensile and the other compressive for the investigated parameters. This is expected given the compression imposed on the material during compaction. In addition, increased compaction density results in larger magnitude of residual stresses. Increased density results from higher compaction and hence larger compressive forces. Similar behaviour is also observed for residual maximum shear stresses (Tau Max) although with let dramatic variation. The minimum principal residual stress (Sigma 2) of -79 MPa was recorded for a compaction density of 83%. Furthermore, a decrease in density is accompanied by progressively larger residual stresses.

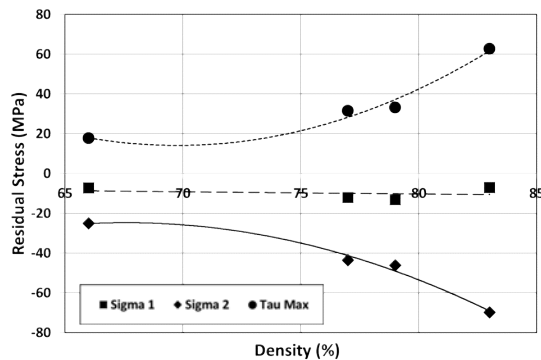


Figure 5: Principal stress variations as a function of compaction density

4. Conclusions

This paper has presented an investigation of the effect of direct powder rolling parameters on the residual stresses induced in green titanium powder compacts. Specimens were prepared by direct rolling of Ti6Al4V at a rotational speed of 10 rpm while varying the rolling gap (0.1, 0.3 and 0.5 mm) and the strip width (0, 50 and 100 mm). Challenges observed with compaction at roll gap of 0.3 and 0.5 mm led to residual stress measurements for specimens prepared with a roll gap of 0.1 mm. Density of the specimens was measured prior to surface residual stress measurements using the XRD technique. Residual stresses were measured at surface locations to give an average surface residual stress for each component. Based on the obtained results, the following conclusions can be made:

1. The residual stresses results were found to be largely compressive for all specimens.
2. The residual stress component in the thickness direction was found to be negligible at the surface.
3. The maximum principal residual stress (in magnitude) recorded was -55 MPa which corresponded to specimen with compaction density of 83%.
4. A decrease in density resulted in residual stresses becoming less compressive.
5. Residual stresses induced in green compacts after compaction are significantly dependent on the process parameters.

The current study does not yield conclusive answers regarding the effect of the stresses on the compacts as measurements were made at a single point. Therefore, more detailed study of residual stress distributions on the surface of the specimen across the whole width, length and thickness is recommended. This could yield more insight into the potential benefits or consequences of having residual stresses from roll compaction.

Acknowledgements

The authors would like to acknowledge NECSA for carrying out the XRD residual stress measurements.

References

- [1] X., Xu, G. L., Nash, and P., Nash, Sintering mechanisms of blended Ti6Al4V powder from diffusion path analysis, *Journal of Materials Science*, Vol. 49, No. 3, 2013, pp.994–1008. Available at: <http://link.springer.com/10.1007/s10853-013-7775-x> [Accessed May 28, 2014].
- [2] V. A. R., Henriquesa, P. P., de Camposa, C. A. A., Cairoa, and J. C., Bressianib, Production of Titanium Alloys for Advanced Aerospace Systems by Powder Metallurgy, *Materials Research*, Vol. 8, No. 4, 443-446, 2005
- [3] C., Leyens and M., Peters, Titanium and Titanium Alloys. Fundamentals and Applications, Wiley-VCH, 2003
- [4] Adams, J.W. et al., Low Cost Titanium Powder Metallurgy Components for Armor and Structural Applications, 1890
- [5] Froes, F.H. et al., The Technologies of Titanium Powder Metallurgy on Mechanical, *The Journal of The Minerals, Metals & Materials Society (TMS)*, Vol. 56, No. 11, 2004, pp 46–48
- [6] S. Chikosha, T. C. Shabalala and H. K. Chikwanda, Effect of particle morphology and size on roll compaction of Ti-based powders, *Powder Technology*, Vol. 264, 2014, Pages 310–319
- [7] D. Cantin, D. Ritchie, M. Gibson, and M. Yousuff, Direct Rolling of Titanium and Titanium Alloy Powders, CSIRO, Available on: <http://www.tida.co.nz/upload/files/13---Delphine-Cantin---CSIRO,-Australia.pdf>
- [8] N. Stone, D. Cantin, M. Gibson, S. Lathabai, D. Ritchie, R. Wilson, R. Rajakumar, and K. Rogers, A Continuous Process for Production of Cp Titanium Sheet By Direct Powder Rolling, *Mater. Sci. Eng.*, 2009.
- [9] V. A. D. Vladimir S. Moxson, Process of Direct Powder Rolling of Blended Titanium Alloys, Titanium Matrix Composites and Titanium Aluminides, United States of America Patent 7311873, 25 December 2007.
- [10] K. Biswas, Comparison of various plasticity models for metal powder compaction processes, *Journal of Materials Processing Technology*, vol. 166, 2004, pp. 107-115.
- [11] I. Askefi, S. Iyer, H. P. Lee and A. M. Cuitino, A quantitative correlation of the effect of density distributions in roller-compacted ribbons on the mechanical properties of tablets using ultrasonics and X-ray tomography, *American Association of Pharmaceutical Scientists*, Vol. 12, No. 3, 2011, pp. 834-853.
- [12] S. E. Schoenberg, D. J. Green, and G. L. Messing, Effect of Green Density on the Thermomechanical Properties of a Ceramic During Sintering, *Journal of the American Ceramic Society*, Vol. 89, No. 8, 2006, pp. 2448–2452.
- [13] S. E. Schoenberg, D. J. Green, A. E. Segall, A. S. Grader, P. M. Halleck and G. L. Messing, Stress and distortions due to green density gradients during densification, *Journal of American Ceramic Society*, Vol. 89, No. 10, 2006, pp. 3027-3033.
- [14] R. Zhou, L. H. Zhang, Y. H. Liu, "Investigation of Residual Stress in Green Compacts of Metal Powder Using X-Ray Diffraction", *Advanced Materials Research*, Vols. 554-556, pp. 461-464, 2012

- [15] Rui Zhou, Lian-hong Zhang, Bai-yan HE, Yu-hong LIU, Numerical simulation of residual stress field in green power metallurgy
- [16] D. Ulutan and T. Ozel., "Machining induced surface integrity in titanium and nickel alloys: a review," *International Journal of Machine Tools and Manufacture*, Vol 5, pp. 50-80, 2011
- [17] Vishay Precision Group, Measurement of residual stresses by hole-drilling strain gauge method, Vishay Precision Group, Technical Note, 2010
- [18] S. Dreier and B. Denkena, Determination of residual stresses in a plate by layer removal with machine-integrated measurement, *Procedia CIRP*, Vol. 24, 2014
- [19] P. S. Prevey, "Current applications of X-ray diffraction residual stress measurement," *Lambda Research*, 1996.
- [20] M. T., Hutchings and A. D., Krawitz, Measurement of residual and applied stress using neutron diffraction, Springer, 1996.
- [21] C. Genzel, I. A. Denks, J. Gibmeier, M. Klaus and G. Wagener, The materials science synchrotron beamline EDDI for energy-dispersive diffraction analysis, *Nuclear Instruments and Methods in Physics Research A*, Vol. 578, 2007, pp. 23-33.
- [22] S. -H., Joo, H. -J., Chang, W. H. Bang, H. N., Han, and K. H., Oh, Analysis of alligatoring behavior during roll pressing of DRI powder with flat roller and indentation-type roller, *Materials Science Forum*, Vol. 475, 005, pp. 3223-3226.